



ELSEVIER

Nuclear Instruments and Methods in Physics Research B 181 (2001) 593–597

NIM B
Beam Interactions
with Materials & Atoms

www.elsevier.com/locate/nimb

Manganese profiles in freshwater mussel shells

R. Siegele^{*}, I. Orlic, D.D. Cohen, S.J. Markich, R.A. Jeffree

Australian Nuclear Science and Technology Organisation, PMB 1, Menai, NSW 2234, Australia

Abstract

The heavy ion microprobe in combination with particle-induced X-ray emission was used to measure the distribution of manganese in freshwater mussel shells (*Hyridella depressa*) from the Nepean river in south-eastern Australia. Close to the ventral edge, bands with an elevated manganese content have been detected. These are correlated with growth bands in the mussels containing increased amounts of organic material, relative to the calcium carbonate matrix. Calcium minima, which were correlated to the annual growth rings, were measured close to the umbo region of the shells. Crown Copyright © 2001 Published by Elsevier Science B.V. All rights reserved.

1. Introduction

Previous studies [1] have shown that the daily micro-laminations in the shells of freshwater bivalves can reflect enhanced concentration of manganese in the aquatic medium during their deposition. Therefore, these shells may be useful as environmental archives of trace element contamination of their aquatic environment. The larger growth increments of bivalve shells resemble the annual rings in trees, where dark and light coloured bands represent different growth rates during the changing seasons. The shells are composed of calcium carbonate (aragonite) crystals, embedded in organic material. The ratio of organic to inorganic matter in the shells can vary seasonally and is typically higher in winter, when the growth slows down. Nyström et al. [2] found strong sea-

sonal growth variations in pearl mussels (*Margaritifera margaritifera*) collected in Sweden. Up to six times higher manganese concentrations were found during the major growth period in spring compared to winter [2,3]. Besides these seasonal variations, strong annual variations have also been reported.

Nyström et al. [2] measured the Mn content in the prismatic layer below the external surface of the shell. Since adult bivalve shells are curved and range in length (from 2 to 20 cm), the sample has to be moved manually between measurements. They further found a 4–5 times higher Mn content in the nacreous layer compared to the prismatic layer (Fig. 1). Since the shell layers near the umbo encompass the whole lifespan of the organism, measuring perpendicular to the surface through these layers is a more efficient way to measure the complete profile in this region, where the shell is only a few millimeters in thickness.

The general aim of this study is to investigate the manganese concentration and its distribution

^{*} Corresponding author. Tel.: +61-2-9717-3967; fax: +61-2-9717 3257.

E-mail address: rns@ansto.gov.au (R. Siegele).

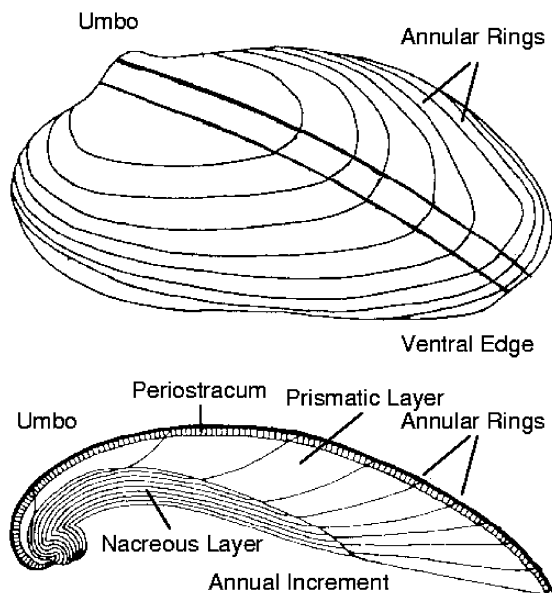


Fig. 1. (a) Shell section cut from the umbo to the posterior ventral edge of the freshwater bivalve shell. (b) Schematic of the cross-section of a shell showing the growth structure of the shell.

in the shell of the freshwater bivalve (*Hyridella depressa*) from the Nepean river in south-eastern Australia. This preliminary study compares Mn measurements taken at various locations in the mussel shell.

2. Experimental

Mussels (*Hyridella depressa*) were sampled from an unpolluted region of the Nepean river about 50 km south-west of Sydney, Australia. The mussels were between 3 and 5 years old. The average concentration of Mn in this part of the river is $40 \mu\text{g l}^{-1}$ [4]. Calcium and manganese in the shell laminations were measured using the Australian Nuclear Science and Technology Organisation (ANSTO) heavy ion microprobe [5].

From each shell, a 3 mm section was cut from the umbo region to the posterior-ventral edge (see Fig. 1(a)). This represents the axis of maximum growth and should therefore yield the most detailed archival information. The sections

were mounted in epoxy resin and polished with diamond paste [6]. First profiles through the whole shell (prismatic and nacreous layer) were taken perpendicular to the surface close to the umbo (see Fig. 1(b)), in order to investigate if it is possible to measure the full record of the environmental exposure of the mussel. These results are complemented with measurements at the ventral edge where the growth rate is highest.

Calcium and manganese in the shells were measured with 9 MeV He^{2+} beams using particle-induced X-ray emission. At this energy the X-ray production and ion range are roughly equivalent to that of 2.2 MeV protons, which results in a high X-ray yield required for this study. Since Ca, the predominant element in the samples, is present at much higher concentrations than Mn, a 700 μm Kapton foil was used to reduce the low-energy X-ray yield. For this filter the Ca yield is reduced by a factor of 500, while the Mn yield is only reduced by a factor of 5. This allows us to increase the He beam current and to measure low Mn concentrations in the calcium carbonate matrix. The X-rays were measured with a Peltier-cooled AMP-TEK X-ray detector with an energy resolution of about 250 eV. The beam was focussed to a spot size of $\approx 3 \mu\text{m}$ and the samples were measured with a He^{2+} beam current of 200 pA.

3. Results and discussion

The cross-section of the mussel shell in Fig. 1(b) shows that in the region close to the umbo the annual growth layers cover the full lifespan of the animal. Therefore, in the first experiment elemental profiles close to the umbo region were measured. Fig. 2(a) shows a typical concentration map of calcium from this region. The map clearly shows bands of lower Ca concentration. Fig. 2(b) shows Ca and Mn profiles taken through the centre of the Fig. 2(a). The Ca profile shows a constant concentration across the shell, with four clear minima. These minima are $\approx 10\text{--}20 \mu\text{m}$ wide and correlate to growth bands visible under the optical microscope. The lower Ca content in these

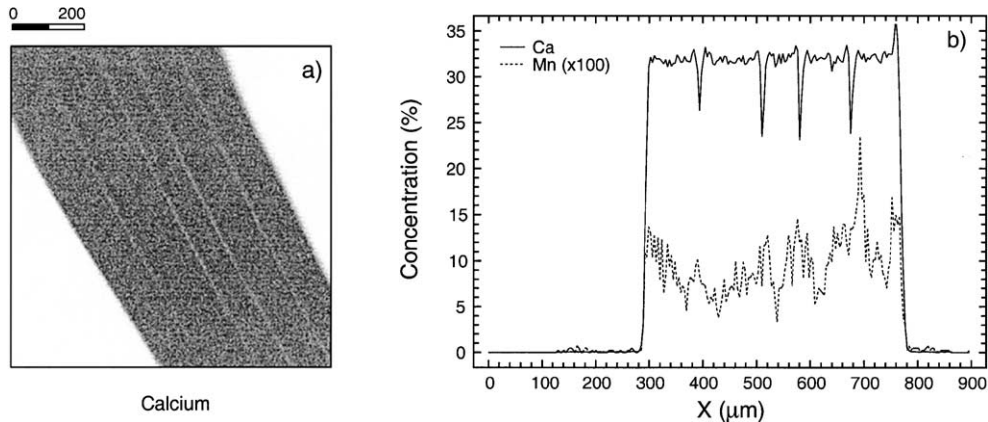


Fig. 2. (a) Calcium map taken close to the umbo region of a shell showing bands of decreased Ca concentration. (b) Calcium and manganese profiles taken through the centre of (a).

bands is due to a higher proportion of organic material. When the water temperature in the Nepean river falls below $\approx 15^{\circ}\text{C}$, bivalves reduce their metabolism and shell growth slows down. During this time more organic material is incorporated into the shell, resulting in a reduced Ca content.

Compared to Ca, the Mn concentration shows marked variations across the shell. In some of the samples, maxima in the Mn concentration appeared to be correlated with a minimum in the Ca concentration, indicating seasonal variations of the Mn concentration.

None of the investigated samples showed an obvious difference in the Mn concentration between prismatic and nacreous layer close to the umbo region as reported by Nyström et al. [2]. This could be due to the different species investigated and climatic differences.

For comparison with the umbonal region of the shell, elemental maps were also taken at the ventral edge. Fig. 3(a) shows a map of the X-ray intensity integrated over the width of the Mn peak in this area. The figure shows a map combined of 4 individual scans spanning ≈ 5 mm, which is equivalent to the annual growth of a young shell. This is the fastest growing part of the shell and thus should represent environmental changes more rapidly. The lower part of the map shows the inside of the shell where new layers are

deposited during the growth process. The upper part of the map shows the external part of the shell. The maps show a band of high X-ray intensity on the upper edge of the shell. This is an artifact of the measurement, caused by Fe contained in the periostracum (organic rich external part) of the shell. The high Fe concentrations are readily visible as a red, rusty colouration on the outside of the shell. Because Fe and Mn X-rays are close in energy, the tail from the strong Fe peak contributes to the Mn yield. This was confirmed by spot measurements taken at the outside edge (A) and the inner part (B) of the shell. The corresponding spectra are shown in Fig. 4. The X-ray spectrum taken at A shows a very high Fe content, while there is no evidence for Mn in this part of the shell. However, the tail of the Fe peak contributes the map in Fig. 3(a) which shows the integral over the region of the Mn peak. In contrast, the spectrum taken in the inner part of the shell at B shows that the intensity is solely due to Mn.

A band of increased Mn concentration is visible on the lower (inside) edge of the shell. This band broadens towards the outer edge of the shell (right), where it fans out into clearly visible individual bands. Along the inside of the shell the width of this band slowly decreases, before it merges into another set of bands that fan out towards the external edge in a similar way. A

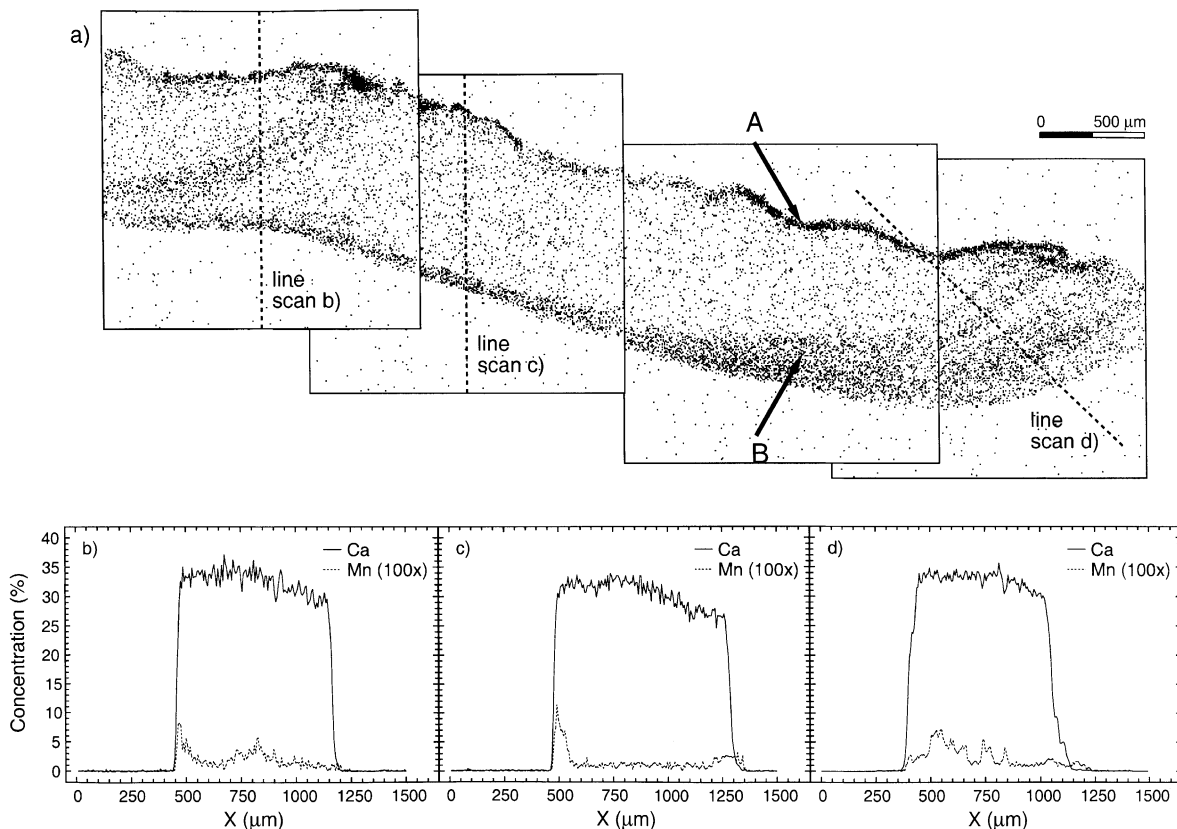


Fig. 3. (a) Manganese map taken at the ventral edge of the shell. The external surface of the shell is at the top of the figure. (b)–(d) Profiles taken at various sections of the shell, as indicated in (a).

micrograph of the same section of the shell is shown in Fig. 5. The micrograph shows dark growth bands correlated with areas of high Mn concentration. These dark bands in the micrograph are regions with an increased organic content, indicating that the Mn is concentrated in organic parts of the shell. Similar results were reported by Nyström et al. [2].

Both the micrograph and the Mn maps illustrate the longitudinal growth process of the shell by adding new layers. The variations in Mn concentration are due to changes in the growth process. At the same time the shell breadth increases, which is a much slower growth process (i.e. growth is three-dimensional).

Profiles through various sections of the shell are shown in Figs. 3(b)–(d). The Mn line scans have been corrected for the contribution from Fe tails.

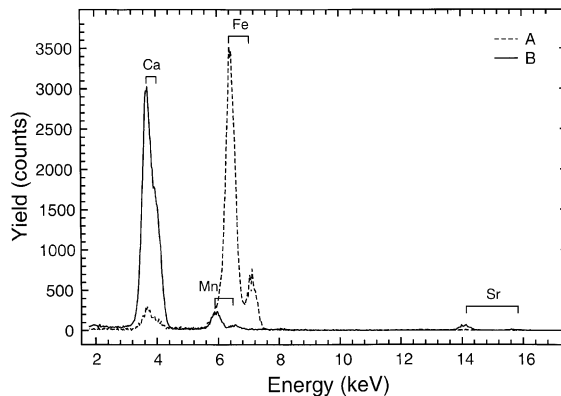


Fig. 4. X-ray spectra taken at the spots A and B indicated in Fig. 3.

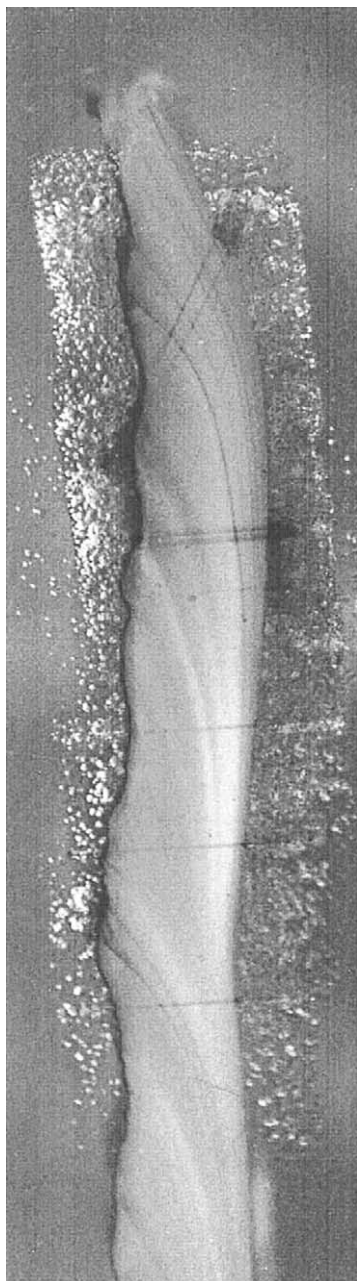


Fig. 5. Optical micrograph from the region shown in Fig. 3. The straight lines across the shell are beam marks caused by the line scans taken across the shell.

This has been done by subtracting the Fe low energy tail from the Mn window using the tail to peak ratio. The profiles of Mn in Figs. 3(b)–(d),

show a Mn baseline of 100–200 ppm, with the Mn increasing to 1000–1500 ppm in the peaks. In contrast, the Mn concentration in the shell adjacent to the umbo is consistently between 800–1500 ppm, never approaching the baseline concentrations of Mn at the ventral edge. However, the Mn concentration close to the umbo is comparable to the concentration in the Mn peaks at the ventral edge. This suggests that the two growth processes result in different Mn concentration within these regions. Profiles further along the shell show that the region with a high Mn concentration slowly increases in thickness.

4. Conclusions

Close to the umbo the Ca concentration shows clear seasonal minima, caused by an increased organic content. This is due to a slower growth process during the colder months of the year. Considerable differences were found in the Mn concentrations, as well as the Mn profiles, in areas close to the umbo and ventral edge. Manganese profiles close to the umbo did not show any structure related to the growth rings, while profiles at the ventral edge show increased Mn concentration correlated to the growth rings. The overall Mn concentration in the umbo region is much higher and is comparable to the concentration in Mn maxima at the ventral edge. Changes in the Mn concentration at the ventral edge of the shell are correlated with seasonal changes.

References

- [1] B. Carell, S. Forberg, E. Grundelius, L. Henrickson, A. Johnels, U. Lindh, H. Mutvei, M. Olsson, K. Svårdström, T. Westermark, *Ambio* 16 (1987) 2.
- [2] J. Nyström, U. Lindh, E. Dunca, H. Mutvei, *Nucl. Instr. and Meth. B* 104 (1995) 612.
- [3] U. Lindh, H. Mutvei, T. Sunde, T. Westermark, *Nucl. Instr. and Meth. B* 30 (1988) 388.
- [4] S.J. Markich, P.L. Brown, *Sci. Total Environ.* 217 (1998) 201.
- [5] R. Siegele, D.D. Cohen, N. Dytlewski, *Nucl. Instr. and Meth. B* 158 (1999) 31.
- [6] R.A. Jeffree, S.J. Markich, F. Lefebvre, M. Thellier, C. Ripoll, *Experimenta* 51 (1995) 839.